

Dynamically emergent correlations in a Brownian gas with diffusing diffusivity

Nikhil Mesquita

Raman Research Institute, Bangalore 560080, India
Email: nikhilm@rrimail.rrri.res.in

Satya N. Majumdar

LPTMS, CNRS, Université Paris-Sud, Université Paris-Saclay, 91405 Orsay, France
Email: satyanarayan.majumdar@cnrs.fr

Sanjib Sabhapandit

Raman Research Institute, Bangalore 560080, India
Email: sanjib@rrri.res.in

Abstract. We study a gas of N Brownian particles in the presence of a common stochastic diffusivity $D(t) = B^2(t)$, where $B(t)$ represents a one-dimensional Brownian motion at time t . Starting with all the particles from the origin, the gas expands ballistically. We show that because of the common stochastic diffusivity, the expanding gas gets dynamically correlated, and the joint probability density function of the position of the particles has a conditionally independent and identically distributed (CIID) structure that was recently found in several other systems. The special CIID structure allows us to compute the average density profile of the gas, extreme and order statistics, gap distribution between successive particles, and the full counting statistics (FCS) that describes the probability density function (PDF) $H(\kappa, t)$ of the fraction of particles κ in a given region $[-L, L]$. Interestingly, the position fluctuation of the central particles and the average density profiles are described by the same scaling function. The PDF describing the FCS has an essential singularity near $\kappa = 0$, indicating the presence of particles inside the box $[-L, L]$ at all times. Near the upper limit $\kappa = 1$, the scaling function $H(\kappa, t)$ has a rather unusual behavior: $H(\kappa, t) \sim (1 - \kappa)^{\beta(t)}$ where the exponent $\beta(t)$ changes continuously with time. While at early times $\beta(t) < 0$ indicating a divergence of $H(\kappa, t)$ as $\kappa \rightarrow 1$, $\beta(t)$ becomes positive for $t > t_c$ where t_c is computed exactly. For $t > t_c$, the scaling function $H(\kappa, t)$ vanishes as $\kappa \rightarrow 1$, indicating that it is highly unlikely to have all the particles in the interval $[-L, L]$. Exactly at $t = t_c$, $\beta = 0$, indicating that the PDF approaches a non-zero constant as $\kappa \rightarrow 1$. Thus, as a function of t , the FCS exhibits an interesting shape transition.

Contents

1 Introduction

<i>Dynamically emergent correlations in a Brownian gas with diffusing diffusivity</i>	2
2 The JPDF and the CIID structure	5
3 Correlation functions	8
4 Average density profile of the gas	9
5 Order Statistics	10
5.0.1 Position fluctuation of the central particles ($\alpha = 0.5$):	12
5.0.2 Distribution of extreme values:	13
6 Gap statistics	15
7 Full Counting Statistics	16
8 Conclusion	18
9 Acknowledgements	20

1. Introduction

A system of non-interacting particles may become dynamically correlated when the particles are coupled to a stochastically fluctuating environment. These correlations emerge dynamically, and are not built in, i.e., they get generated even though there is no direct interaction between the particles. These correlations emerge because the particles share the same fluctuating environment. Such dynamically emerging correlations have recently been uncovered theoretically in a number of simple models [1–4] and have also been demonstrated experimentally [5]. In all the theoretical models studied so far, the fluctuating environment drives the system into a nonequilibrium stationary state (NESS) in which there is an all-to-all effective attraction between the particles, which makes them strongly correlated. This includes, e.g., N non-interacting Brownian particles that are simultaneously reset to the origin at a constant rate [1,2], and also N particles in a harmonic trap, whose stiffness fluctuates between two values with rates r_1 and r_2 [3], or the center of the trap undergoes a stochastic modulation [4]. Such a strongly correlated NESS has also been found in a quantum system consisting of N non-interacting bosons in a harmonic trap subjected to a specific quantum resetting protocol [6].

However, in some systems, the fluctuating environment may not drive the system into a NESS, and the state of the system is always time-dependent. It is interesting to ask how the correlations between the particles grow with time in such time-dependent systems. In this paper, we present an exactly solvable model with such time-dependent emergent correlations created by the fluctuating environment. Our model is just an N -body generalization of a well-studied single Brownian particle subjected to a diffusing diffusivity. More precisely, we consider N non-interacting Brownian particles on a line with coordinates $\{x_1(t), x_2(t), \dots, x_N(t)\}$ that evolve as

$$\frac{dx_i}{dt} = \sqrt{2D(t)} \eta_i(t), \quad (1)$$

where $D(t) > 0$ represents a fluctuating positive diffusivity, which itself performs an independent stochastic motion. The set $\{\eta_1(t), \eta_2(t), \dots, \eta_N(t)\}$ represents independent white noises with zero mean with a correlator $\langle \eta_j(t) \eta_k(t') \rangle = \delta_{j,k} \delta(t-t')$. The dynamics of $D(t)$ is not affected by the dynamics of $x_i(t)$'s. However, the dynamics of $x_i(t)$'s for each i share the common fluctuating diffusivity $D(t)$, which makes them correlated. The dynamics of a single particle ($N = 1$) for different choices of $D(t) > 0$, such as the square of a one-dimensional Brownian motion or a one-dimensional Ornstein-Uhlenbeck (OU) process, have been studied in the literature [7–21]. In fact, the above model of N non-interacting Brownian particles with a common fluctuating diffusing diffusivity $D(t)$ is equivalent to an N -dimensional Brownian motion with diffusing diffusivity, for which the PDF of the radial coordinate $R = \sqrt{x_1^2 + x_2^2 + \dots + x_N^2}$ has been studied for $D(t) = B^2(t)$ [22], where $B(t)$ represents a one-dimensional Brownian motion at time t , i.e.,

$$\frac{dB}{dt} = \sqrt{2\Lambda^2} \chi(t), \quad \text{with } B(0) = 0. \quad (2)$$

Here $\Lambda > 0$ is a constant that has the dimension of velocity and $\chi(t)$ is a Gaussian white noise with zero mean and two-time correlation function $\langle \chi(t)\chi(t') \rangle = \delta(t - t')$. The choice of stochastic diffusivity $D(t) = B^2(t)$ might model a medium undergoing heating where one expects the amplitude of the random force driving the Brownian particle typically increases with time, but in a fluctuating manner. It was found that (i) the typical R grows linearly with time and (ii) the PDF of the scaled distance R/t has a universal exponential tail in all dimensions N with the dependence on N appearing only through the subleading prefactor [22]. However, in this paper, we are interested in observables such as the average density, the order statistics, the gap statistics, and the full counting statistics. These observables make sense only if we interpret $x_i(t)$'s as the position of N independent particles on a line, rather than interpreting them as the components of the position of a single particle in N dimensions. For example, the gap between two consecutive particles makes sense only in one dimension, since there is no physical meaning of the gap between two components of a single vector in N dimensions.

Let us also remark that another interesting recent example of diffusing diffusivity—specifically with the choice $D(t) = B^2(t)$ —has been studied in the context of a Rouse polymer chain, or equivalently, a Gaussian interface evolving according to the Edwards–Wilkinson equation [23]. It was found that the typical height at a fixed point in space grows as $t^{3/4}$ at late times. Moreover, the scaled height approaches a highly non-trivial non-Gaussian distribution that was computed exactly [23]. In this Rouse model, the monomers have pairwise harmonic interactions between them. The model that we consider here is even simpler. Unlike the interacting monomers in the Rouse chain, here the particles have no direct interaction between them. They only share the common diffusivity, which we choose to be $D(t) = B^2(t)$, as in the Rouse chain or the interface model above. Our goal in this paper is to see how the correlations between particles emerge dynamically from sharing the same time-dependent fluctuating diffusivity $D(t) = B^2(t)$ and, moreover, how these correlations affect the behavior of different physical observables of this gas of particles. This is done exactly by computing the joint probability density function (JPDF) $P(x_1, x_2, \dots, x_N, t)$ at any time t . Furthermore, we show that this JPDF in our model at any time t also has a *conditionally independent and identically distributed* (CIID) structure found recently in a number of other models [1–4, 6, 24]. This special CIID structure allows the exact computation of various macroscopic and microscopic observables. The average density profile $\rho(x, t)$ of the gas at time t is an example of a macroscopic observable. Microscopic observables include the extreme and the order statistics, the gap statistics, and the full counting statistics. These observables have been computed recently for other models mentioned above with a CIID structure in the steady state [1–4, 6, 24]. The difference in our case is that we do not have a steady state for the choice $D(t) = B^2(t)$, and hence these observables are time dependent. Nevertheless, exploiting the CIID structure, these observables can be computed exactly at all times t .

The rest of the paper is organized as follows. We first obtain the JPDF in section 2 and show that it has the CIID structure. Using the JPDF, we compute the other

observable in the subsequent sections. In section 3, we compute the correlations between the particles and show that there are strong positive correlations between the particles, characterized by the correlation function $\langle x_i^2 x_j^2 \rangle - \langle x_i^2 \rangle \langle x_j^2 \rangle$ that increases as t^4 with time. In fact, the gas in our model expands ballistically with time with a length-scale $\xi(t) \propto t$, and in section 4 we find the density profile of the gas by scaling the space with $\xi(t)$. Section 5 contains the order statistics where we investigate the distribution of the k -th maximum. The two special cases $k = N/2$ and $k = 1$ are treated more carefully in sub-sections 5.0.1 and 5.0.2 respectively. In section 6 we consider the gap statistics, and finally section 6.8 contains the full counting statistics. We conclude in section 8.

2. The JPDF and the CIID structure

We start by computing the exact JPDF $P(x_1, x_2, \dots, x_N, t)$ of the positions of the particles at any time t . Assuming that $x_i(0) = 0$ for all i , it follows from (1) that

$$x_i(t) = \int_0^t \sqrt{2D(\tau)} \eta_i(\tau) d\tau. \quad (3)$$

Hence, for any given realization of the fluctuating diffusivity process $\{D(\tau); 0 \leq \tau \leq t\}$, the process $\{x_1(t), x_2(t), \dots, x_N(t)\}$ is an independent multivariate Gaussian process with a JPDF

$$P(x_1, x_2, \dots, x_N, t | \{D(\tau)\}) = \prod_{j=1}^N \frac{1}{\sqrt{2\pi V(t)}} \exp\left(-\frac{x_j^2}{2V(t)}\right), \quad (4)$$

where the variance $V(t)$ of x_i for any i and given the realization of $\{D(\tau); 0 \leq \tau \leq t\}$ is given by the functional

$$V(t) = 2 \int_0^t D(\tau) d\tau, \quad (5)$$

which is easily computed from (3) using the properties of the white noise, namely, $\langle \eta_j(\tau) \rangle = 0$ and $\langle \eta_j(\tau) \eta_k(\tau') \rangle = \delta_{j,k} \delta(\tau - \tau')$. Note that the dependence of the JPDF in (4) on the realization of $\{D(\tau); 0 \leq \tau \leq t\}$ appears only through $V(t)$, which is an integral over $2D(\tau)$. Hence, averaging JPDF in (4) over the realization of the full process $\{D(\tau); 0 \leq \tau \leq t\}$ amounts to averaging over the random variable $V(t)$ given in (5).

$$P(x_1, x_2, \dots, x_N, t) = \int_0^\infty P(x_1, x_2, \dots, x_N, t | \{D(\tau)\}) h(V, t) dV \quad (6)$$

where $h(V, t)$ denotes the PDF of the random variable V at time t .

With the choice $D(\tau) = B^2(\tau)$, the variance $V(t)$ in (5) can be interpreted as a Brownian functional

$$V(t) = 2 \int_0^t B^2(\tau) d\tau, \quad (7)$$

where $B(\tau)$ is a Brownian motion defined in (2). Then, averaging (4) over V , the JPDP of the position of the particles at any time t is given by

$$P(x_1, x_2, \dots, x_N, t) = \int_0^\infty dV h(V, t) \prod_{j=1}^N \frac{1}{\sqrt{2\pi V}} \exp\left(-\frac{x_j^2}{2V}\right), \quad (8)$$

where the only unknown so far is the PDF $h(V, t)$ of V defined in (7).

The PDF $h(V, t)$ of the functional of the square of a Brownian motion defined in (7) has been long known in the mathematics literature [25–28] — also see [22, 29] for a physicist’s derivation. Its Laplace transform, with $B(t)$ defined in (2), is given by

$$\tilde{h}(\lambda, t) = \int_0^\infty e^{-\lambda V} h(V, t) dV = \sqrt{\operatorname{sech}(2\Lambda t \sqrt{2\lambda})}. \quad (9)$$

Therefore, formally, $h(V, t)$ is given by the Bromwich integral

$$h(V, t) = \frac{1}{2\pi i} \int_{\gamma_1 - i\infty}^{\gamma_1 + i\infty} d\lambda e^{\lambda V} \tilde{h}(\lambda, t) = \frac{1}{2\pi i} \int_{\gamma_1 - i\infty}^{\gamma_1 + i\infty} d\lambda e^{\lambda V} \sqrt{\operatorname{sech}(2\Lambda t \sqrt{2\lambda})}, \quad (10)$$

where γ_1 is a real constant such that all the singularities of the function $\tilde{h}(\lambda, t)$ lie on the left of the contour in the complex λ plane. It follows from (7) that since typically $B(\tau)$ scales as $\sqrt{\tau}$, the quantity $V(t)$ scales as t^2 for any t . Consequently, one expects that $h(V, t)$ must have a scaling form $h(V, t) \sim t^{-2} q(V/t^2)$. Actually, it turns out to be convenient to write the PDF in the scaling form

$$h(V, t) = \frac{1}{[\xi(t)]^2} Q\left(\frac{V}{[\xi(t)]^2}\right), \quad \text{with} \quad \xi(t) = \sqrt{2} \Lambda t, \quad (11)$$

where the scaling function $Q(z)$ can be read off from (10) as

$$Q(z) = \frac{1}{2\pi i} \int_{\gamma - i\infty}^{\gamma + i\infty} ds e^{sz} \sqrt{\operatorname{sech}(2\sqrt{s})}. \quad (12)$$

Here γ is a real constant such that all the singularities of $\sqrt{\operatorname{sech}(2\sqrt{s})}$ lie on the left of the contour in the complex s plane. While it is hard to perform the integral in (12) exactly, it can be easily analyzed to extract the small and large z behaviors of the function $Q(z)$.

To obtain the small z behavior, it is useful to express the $\sqrt{\operatorname{sech}(2\sqrt{s})} = \sqrt{2} e^{-\sqrt{s}} / \sqrt{1 + e^{-4\sqrt{s}}}$ in (12) and then expand the denominator using the binomial series, as

$$Q(z) = \sqrt{2} \sum_{n=0}^{\infty} \binom{-1/2}{n} \int_{\gamma - i\infty}^{\gamma + i\infty} \frac{ds}{2\pi i} e^{zs} e^{-(4n+1)\sqrt{s}}. \quad (13)$$

The evaluation of the Bromwich integral in (13) for any n — where the integrand has a branch-point at $s = 0$ — is quite standard. The inverse Laplace transform yields,

$$Q(z) = \frac{1}{\sqrt{2\pi}} \sum_{n=0}^{\infty} \binom{-\frac{1}{2}}{n} \frac{4n+1}{z^{3/2}} \exp\left[-\frac{(4n+1)^2}{4z}\right]. \quad (14)$$

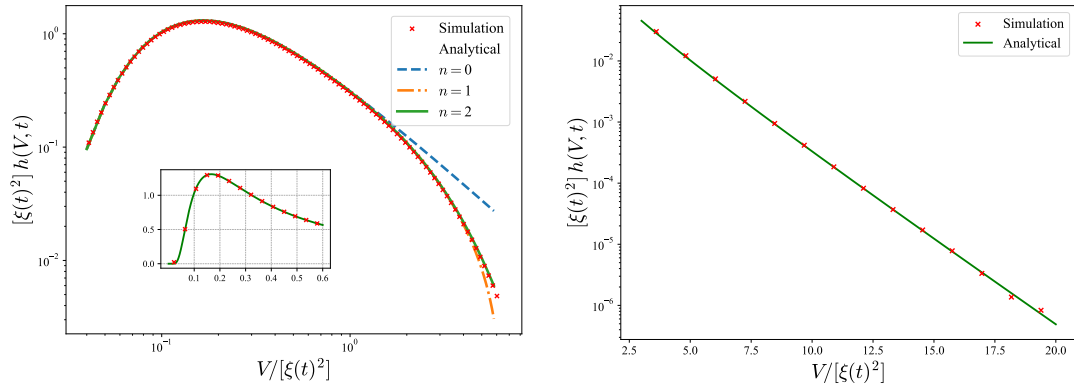


Figure 1. The PDF $Q(V/[\xi(t)]^2) \equiv [\xi(t)]^2 h(V, t)$ of the scaled variable $V/[\xi(t)]^2$. The points are from numerical simulations for the parameters $\Lambda = 1$, $dt = 0.01$, $t = 10$, averaged over 10^8 realizations. The left panel highlights the small z behavior while the right one highlights the tail behavior. Left: The solid lines are analytical plots for different truncations of the infinite series in equation (14). Right: The solid line plots the asymptotic tail given in (15).

While the infinite series in (14) is an exact expression of $Q(z)$, it is mostly useful for describing the small z behavior, by keeping only a few terms of the series, as shown in the left panel in figure 1.

On the other hand, to extract the large z behavior, we analyze (12) directly. We note that the function $\text{sech}(2\sqrt{s})$ has simple poles on the negative real axis at $s_n = -(2n+1)^2\pi^2/16$ with $n = 0, 1, 2, \dots$. Therefore, large z behavior of $Q(z)$ can be obtained by only retaining the closest branch point to the origin $s_0 = -\pi^2/16$ of the integrand in (12), i.e.,

$$Q(z) \sim \frac{\sqrt{\pi}}{2} \int_{\gamma-i\infty}^{\gamma+i\infty} \frac{ds}{2\pi i} \frac{e^{sz}}{\sqrt{s + \pi^2/16}} = \frac{1}{2\sqrt{z}} \exp\left(-\frac{\pi^2 z}{16}\right). \quad (15)$$

We compare this asymptotic exponential tail behavior of $Q(z)$ in (15) with numerical simulations in figure 1 and find excellent agreement.

To summarize, the JPDF $P(x_1, x_2, \dots, x_N, t)$ for the positions of the N particles in our stochastically heated Brownian gas with a common fluctuating diffusivity $D(t) = B^2(t)$ has the CIID structure given in (8), where the PDF $h(V, t)$ of the Brownian functional $V(t)$, given in (7), has the scaling form given in (11), with the scaling function $Q(z)$ given in (12). The scaling function $Q(z)$ is given by the exact infinite series in (14) and has the following limiting behaviors

$$Q(z) \sim \begin{cases} \frac{1}{\sqrt{2\pi} z^{3/2}} e^{-1/(4z)} & \text{for } z \rightarrow 0, \\ \frac{1}{2\sqrt{z}} e^{-\pi^2 z/16} & \text{for } z \rightarrow \infty. \end{cases} \quad (16)$$

Now, given the CIID structure in (8), we next proceed to compute various

macroscopic and microscopic observables. In particular, motivated by earlier studies [1–4, 6], we compute the following observables:

- (i) Correlation between the particles.
- (ii) The average density profile of particles $\rho(x, t)$.
- (iii) The distribution of the maximum displacement $M_1 = \max[x_1(t), x_2(t), \dots, x_N(t)]$, called the extreme value distribution.
- (iv) The distribution of the k -th largest displacement M_k , called the order statistics.
- (v) The distribution of the spacing between successive particles $g = M_k - M_{k+1}$, called the gap statistics.
- (vi) The distribution of the number of particles in the domain $[-L, L]$, called the full counting statistics (FCS).

3. Correlation functions

The CIID structure in (8) makes it immediately evident that the random variables $\{x_1, x_2, \dots, x_N\}$ are correlated, as the JPDF is not a product of the marginal distributions of each variable. Nevertheless, let us explicitly compute the correlations between the positions of the particles. Since the JPDF in (4) is symmetric with respect to any x_i for any given $V(t)$, the mean $\langle x_i \rangle|_V$ vanished even before averaging over V , for any i . As a consequence the two-particle correlation function $\langle x_i x_j \rangle - \langle x_i \rangle \langle x_j \rangle$ for $i \neq j$ trivially vanishes. Therefore, to capture the two-particle correlations, we need to go to the next order correlation function $C_{i,j} = \langle x_i^2 x_j^2 \rangle - \langle x_i^2 \rangle \langle x_j^2 \rangle$. This correlation function is easy to compute by using the JPDF in (8), as

$$C_{i,j} = \langle x_i^2 x_j^2 \rangle - \langle x_i^2 \rangle \langle x_j^2 \rangle = \langle V^2(t) \rangle - \langle V(t) \rangle^2 \quad \text{for } i \neq j. \quad (17)$$

Now, using the scaling form (11), it is quite easy to see that the moments of $h(V, t)$ are given by

$$\langle V^n \rangle = [\xi(t)]^{2n} \int_0^\infty z^n Q(z) dz = [\xi(t)]^{2n} (-1)^n \frac{d^n}{ds^n} \sqrt{\text{sech}(2\sqrt{s})} \Big|_{s=0}, \quad (18)$$

where $\xi(t)$ is defined in (11) and we have used (12) for $Q(z)$. In particular, we get the first two moments as

$$\langle V \rangle = [\xi(t)]^2 \quad \text{and} \quad \langle V^2 \rangle = \frac{7}{3} [\xi(t)]^4. \quad (19)$$

Consequently, from (17), we get

$$C_{i,j} = \langle x_i^2 x_j^2 \rangle - \langle x_i^2 \rangle \langle x_j^2 \rangle = \frac{4}{3} [\xi(t)]^4 = \frac{16}{3} \Lambda^4 t^4, \quad (20)$$

where we have used $\xi(t) = \sqrt{2} \Lambda t$ in the last step. Therefore, the particles have strong positive correlations between them, which are dynamically generated by the common fluctuating diffusivity. It also follows from (20) that typical x_i scales as $\xi(t) \sim \Lambda t$, indicating that the typical positions of the particles grow ballistically with t .

4. Average density profile of the gas

The average density of particles at a position x at time t is defined by

$$\rho(x, t) = \frac{1}{N} \left\langle \sum_{n=1}^N \delta(x_n(t) - x) \right\rangle, \quad (21)$$

where the $\langle \cdot \rangle$ represents average evaluated with respect to the JPDF in (8). Since the JPDF in (8) is symmetric with respect to the permutation of the positions variables, from (21) we have $\rho(x, t) = \langle \delta(x_1(t) - x) \rangle$. Therefore, the average density profile is, in fact, the marginal PDF $\int_{-\infty}^{\infty} \cdots \int_{-\infty}^{\infty} P(x, x_2, \dots, x_N) dx_2 \cdots dx_N$,

$$\rho(x, t) = \int_0^{\infty} dV h(V, t) \frac{1}{\sqrt{2\pi V}} \exp\left(-\frac{x^2}{2V}\right), \quad (22)$$

or equivalently, the PDF of the position of a particle for the $N = 1$ case. As we mentioned in the introduction, the position distribution of a single Brownian particle with a fluctuating diffusivity $D(t) = B^2(t)$ has been studied earlier [11, 22, 29], where it was found that the PDF of the position admits the scaling form \ddagger

$$\rho(x, t) = \frac{1}{2\sqrt{2}\xi(t)} f\left(\frac{x}{2\sqrt{2}\xi(t)}\right), \quad (23)$$

with the scaling function given by [22, 29] (also see [11] for an alternative expression),

$$f(y) = \frac{1}{\sqrt{2\pi^3}} \Gamma\left(\frac{1}{4} + iy\right) \Gamma\left(\frac{1}{4} - iy\right). \quad (24)$$

In figure 2, we plot the distribution of the scaled density profile obtained from numerical simulation and compare it with the scaling function $f(y)$ in (24) and find excellent agreement. The scaling function $f(y)$ in (24) has the following limiting behaviors [11, 22, 29]

$$f(y) \sim \begin{cases} \frac{[\Gamma(1/4)]^2}{\sqrt{2\pi^3}} [1 - ay^2 + O(y^4)] & \text{as } y \rightarrow 0 \\ \sqrt{\frac{2}{\pi|y|}} e^{-\pi|y|} & \text{as } |y| \rightarrow \infty. \end{cases} \quad (25)$$

where $[\Gamma(1/4)]^2/\sqrt{2\pi^3} = 1.66925 \dots$ the constant $a = 17.1973 \dots$

It is worth remarking that, indeed, using the scaling form of $h(V, t)$ from (11) in (22) suggests the scaling form in (23) with the scaling function given by

$$f(y) = \frac{2}{\sqrt{\pi}} \int_0^{\infty} dz Q(z) \frac{1}{\sqrt{z}} e^{-4y^2/z}. \quad (26)$$

\ddagger The numerical factor $2\sqrt{2}$ in the scaling form is not important and merely included to have a familiar form of the scaling function based on prior knowledge.

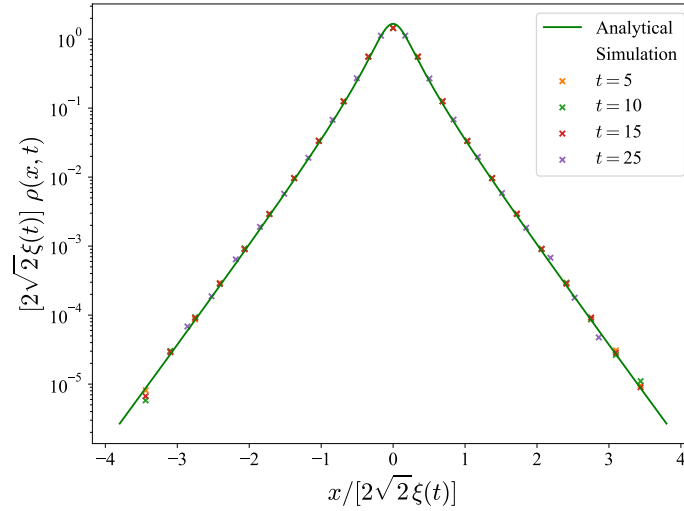


Figure 2. The scaled collapsed plot of the distribution of the average density profile at various times. The solid curve plots the closed form of the analytical scaling function $f(z)$ given in (24). The parameters used in the simulation are $\Lambda = 1$, $dt = 0.01$, and we average over 10^7 realizations.

Now, using the expression of $Q(z)$ from (14) in (26) and integrating over z , we get an alternative expression for the scaling function $f(y)$ as

$$f(y) = \frac{4\sqrt{2}}{\pi} \sum_{n=0}^{\infty} \binom{-\frac{1}{2}}{n} \frac{4n+1}{(4n+1)^2 + 16y^2}. \quad (27)$$

We note that while the small y behavior of $f(y)$ in (25) can be directly obtained from (27) by expanding the summand around $y = 0$ and performing the summation separately for each order in y , the asymptotic tail behavior for large y does not follow from (27) directly. The equivalence between (24) and (27) can be easily established by taking a Fourier transform of (24) and then summing over n , which gives

$$\tilde{f}(k) = \frac{1}{\sqrt{2\pi}} \sqrt{\text{sech}(k/2)}. \quad (28)$$

Now, (28) is nothing but the Fourier transform of the PDF in (27) [29], i.e.,

$$\frac{1}{\pi} \int_0^{\infty} \cos(ky) \sqrt{\text{sech}(k/2)} dk = \frac{1}{\sqrt{2\pi^3}} \Gamma\left(\frac{1}{4} + iy\right) \Gamma\left(\frac{1}{4} - iy\right). \quad (29)$$

5. Order Statistics

Let $M(t) = \{M_1, M_2, M_3, \dots, M_N\}$, be an ordered set that describes, at a particular time t , the displacements of the particles in a descending order, i.e., $M_1 > M_2 > M_3 > \dots > M_N$, such that M_1 denotes the maximum position, M_2 denotes the second maximum and so on. These M_k 's are random variables, and the distribution of these

is called order statistics. The case of $k = 1$ and $k = N$ corresponds to *extreme value statistics* (EVS). Before going to the EVS, we look at the order statistics in the bulk, in the limit $N \rightarrow \infty$ and $k \rightarrow \infty$, keeping $\alpha = k/N \in (0, 1)$. The probability that the k -th element assumes the value w for a particular realization of $\{D(\tau)\}$, i.e., for a given V , is given by [1, 30–32] ,

$$\text{Prob.}(M_k = w|V) = \frac{N!}{(k-1)!(N-k)!} [1 - \psi(w|V)]^{N-k} p(w|V) [\psi(w|V)]^{k-1} , \quad (30)$$

where

$$p(x|V) = \frac{1}{\sqrt{2\pi V}} \exp\left(-\frac{x^2}{2V}\right) \quad [\text{see (8)}] \quad (31)$$

is the conditional PDF of the position of a single particle for a given V (the conditional positions of the particles are independent for a given V), and

$$\psi(w|V) = \int_w^\infty dx' p(x'|V) = \frac{1}{2} \text{erfc}\left(\frac{w}{\sqrt{2V}}\right) \quad (32)$$

is the conditional cumulative distribution. Now using Sterling's approximation for the bulk, one arrives at

$$\text{Prob.}(M_k = w|V) = \sqrt{\frac{N\alpha}{2\pi(1-\alpha)}} \frac{p(w|V)}{\psi(w|V)} e^{-N\phi(w)} , \quad (33)$$

where $\phi(w)$ given by,

$$\phi(w) = \alpha \ln \left[\frac{\alpha}{\psi(w|V)} \right] + (1-\alpha) \ln \left[\frac{1-\alpha}{1-\psi(w|V)} \right] . \quad (34)$$

The cumulative distribution $\psi(w|V)$ in (32) is a monotonically decreasing function of w , with $\psi(w|V) \rightarrow 1$ as $w \rightarrow -\infty$ and $\psi(w|V) \rightarrow 0$ as $w \rightarrow \infty$. Consequently, for any $\alpha \in (0, 1)$, the large deviation function $\phi(w|V)$ is a convex function that diverges at both ends $w \rightarrow \pm\infty$ and has a unique minimum at a particular value $w = q(\alpha, V)$. The location of the minimum can be obtained by setting $\phi'(q) = 0$, which, in turn, gives $\psi(q|V) = \alpha$. Therefore, using the explicit expression from (32), we have

$$q(\alpha, V) = \sqrt{2V} \text{erfc}^{-1}(2\alpha) , \quad (35)$$

where erfc^{-1} is the inverse of the complementary error function. As α varies continuously from 0 to 1, the location of the minimum $q(\alpha, V)$ decreases monotonically from ∞ to $-\infty$, crossing zero at $\alpha = 1/2$.

It is evident from (34) that $\phi(q) = 0$. Moreover, from (34), using (32) and $\psi(q|V) = \alpha$, it is easy to find that $\phi''(q) = [p(q|V)]^2 / [\alpha(1-\alpha)]$. Therefore, expanding $\phi(w)$ around q up to the second order one finds that

$$\text{Prob.}(M_k = w|V) = \sqrt{\frac{N[p(q|V)]^2}{2\pi\alpha(1-\alpha)}} \exp \left[-N \frac{[p(q|V)]^2}{2\alpha(1-\alpha)} (w-q)^2 \right] , \quad (36)$$

where $p(q|V)$ is defined in (31). In the limit $N \rightarrow \infty$, the variance of this Gaussian distribution tends to zero, and it converges to a Dirac delta function,

$$\lim_{N \rightarrow \infty} \text{Prob.}(M_k = w|V) = \delta[w - q(\alpha, V)]. \quad (37)$$

Therefore, averaging over the distribution $h(V, t)$ given in (11), we obtain the unconditional order statistics as

$$\text{Prob.}(M_k = w) = [\xi(t)]^{-2} \int_0^\infty dV Q(V/[\xi(t)]^2) \delta[w - q(\alpha, V)]. \quad (38)$$

Since $q(\alpha, V)$ in (35) is positive for $\alpha \in (0, 0.5)$ and any V , the distribution in (38) is supported over $w \in (0, \infty)$ for $\alpha \in (0, 0.5)$. Similarly, the distribution is supported over $w \in (-\infty, 0)$ for $\alpha \in (0.5, 1)$. Using the explicit expression of $q(\alpha, V)$ from (35), the integral in (38) can be performed explicitly, giving

$$\text{Prob.}(M_k = w) = \frac{|w|}{[\theta_\alpha \xi(t)]^2} Q\left(\frac{w^2}{2[\theta_\alpha \xi(t)]^2}\right), \quad \text{with } \theta_\alpha = \text{erfc}^{-1}(2\alpha), \quad (39)$$

where $Q(z)$ is defined in (14). We compare (39) with numerical simulations in figure 3 and find excellent agreement. We remark that the limiting behavior of $Q(z)$ in (16) translates to the following limiting behaviors of $\text{Prob.}(M_k = w)$ in (39),

$$\text{Prob.}(M_k = w) \sim \begin{cases} \frac{2\xi(t)|\theta_\alpha|}{\sqrt{\pi}w^2} \exp\left(-\frac{[\xi(t)]^2\theta_\alpha^2}{2w^2}\right) & \text{as } |w| \rightarrow 0, \\ \frac{1}{\sqrt{2}\xi(t)|\theta_\alpha|} \exp\left(-\frac{\pi^2 w^2}{32[\xi(t)]^2\theta_\alpha^2}\right) & \text{as } |w| \rightarrow \infty. \end{cases} \quad (40)$$

5.0.1. Position fluctuation of the central particles ($\alpha = 0.5$): The PDF of the k -th position given in (39) is expected to be valid for particles in the bulk. For the special case $\alpha = 1/2$, i.e., for the central particle, from (35) $q(1/2, V) = 0$. Therefore, from (38), the PDF $\text{Prob.}(M_{N/2} = w) \rightarrow \delta(w)$ to the leading order. To obtain the finite N correction for large N , we use (36) with $\alpha = 1/2$ and average over V using $h(V, t)$ from (11),

$$\text{Prob.}(M_{N/2} = w) = \frac{\sqrt{N}}{\pi} \int_0^\infty dV \frac{Q(V/[\xi(t)]^2)}{[\xi(t)]^2 \sqrt{V}} \exp\left[-\frac{Nw^2}{\pi V}\right], \quad (41)$$

where we have used $p(0|V) = 1/\sqrt{2\pi V}$. Making a change of variable $z = V/[\xi(t)]^2$ gives,

$$\text{Prob.}(M_{N/2} = w) = \frac{\sqrt{N}}{\pi \xi(t)} \int_0^\infty dz \frac{Q(z)}{\sqrt{z}} e^{-4y^2/z} \quad \text{with } y = \frac{\sqrt{N}w}{2\sqrt{\pi}\xi(t)}. \quad (42)$$

Now we note that the integral in (42) is the same as in (26). Therefore, after evaluating the integral, we get

$$\text{Prob.}(M_{N/2} = w) = \frac{\sqrt{N}}{2\sqrt{\pi}\xi(t)} f\left(\frac{\sqrt{N}w}{2\sqrt{\pi}\xi(t)}\right), \quad (43)$$

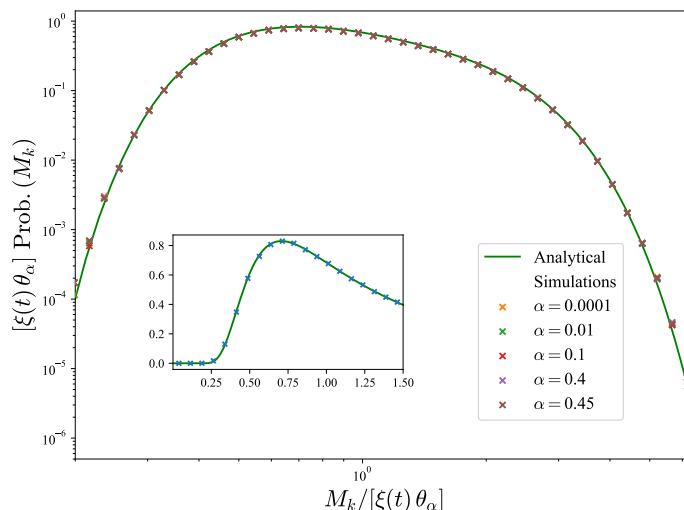


Figure 3. The PDF of the scaled variable $M_k/[\xi(t)\theta_\alpha]$ for various $\alpha = k/N$. The points represent the simulation data for parameters $\Lambda = 1$, $dt = 0.01$, $t = 4$, $N = 10^6$, and averaged over 10^6 realizations. The solid curve is the analytical scaling function $Q(z)$ described in equation (39). The inset shows the essential singularity of the distribution near zero.

where the scaling function $f(z)$ is given in (24). The asymptotic form of the scaling function $f(y)$ in (25) gives an exponential tail for the PDF (43) of the position of the central particle,

$$\text{Prob.}(M_{N/2} = w) = \left(\frac{\sqrt{\pi N}}{\xi(t)} \right)^{\frac{1}{2}} \frac{1}{\pi \sqrt{|w|}} \exp \left(-\frac{\sqrt{\pi N}}{2 \xi(t)} |w| \right). \quad (44)$$

In figure 4, we compare (43) with numerical simulations and find excellent agreement. The typical width of the distribution $\sqrt{\langle w^2 \rangle} \sim \xi(t)/\sqrt{N}$ tends to zero in the limit $N \rightarrow \infty$ for any finite t , forcing the distribution in (43) to a Dirac delta function.

It is interesting to note that the scaling function $f(y)$ in (43) describing the PDF of the position of the middle particle is exactly the same as the scaling function that appears in the average density profile in (23). Mathematically, this universality arises because of the equivalence of the integrals in (26) and (42), for any $Q(z)$. The function $Q(z)$, of course, depends on specific models, resulting in different forms of $f(y)$ for different models. For example, $Q(z) = re^{-rz}$ for a Brownian gas correlated by resetting [1], whereas it has a different expression for a Brownian gas correlated via a switching harmonic trap [3]. Nevertheless, the equivalence between the position distribution of the central particle and the average density profile remains valid for a large class of models where the JPDF has the particular CIID structure given in (8).

5.0.2. Distribution of extreme values: Let us now look into the distribution of the position of the rightmost particle $M_1 = \max(\{x_1, x_2, \dots, x_N\})$ separately. It is more convenient to consider the cumulative distribution of M_1 . The probability that $M_1 < w$

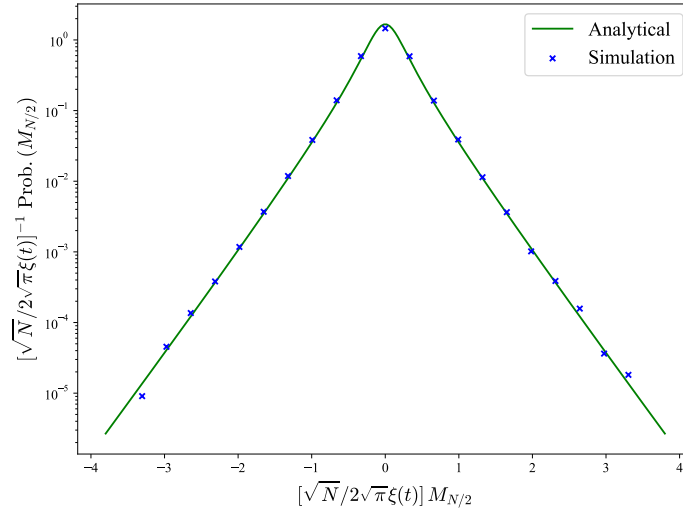


Figure 4. The PDF of the central particle with the appropriate scaling. The points represent the simulation data for the parameters $\Lambda = 1$, $dt = 0.01$, $t = 4$, $N = 10^6$, and averaged over 10^6 realizations. The solid line plots the closed form of the scaling function $f(z)$ given in equation (24).

is mathematically equal to the probability that all the positions $\{x_1, x_2, \dots, x_N\}$ are less than the value w . The latter, for a given realization of the diffusion coefficient, i.e., for a given V , can be expressed as [30–33]

$$\text{Prob.}(M_1 < w|V) = [1 - \psi(w)]^N, \quad (45)$$

where $\psi(w)$ is given in (32). Since $\psi(w) \rightarrow 0$ for $w \rightarrow \infty$, taking the limit $w \rightarrow \infty$ and $N \rightarrow \infty$, keeping $N\psi(w) \sim O(1)$, we get

$$\text{Prob.}(M_1 < w|V) \rightarrow \exp[-N\psi(w)]. \quad (46)$$

For large N , we expect the typical location of the maximum $\sqrt{2V}a_N$ to be such that the argument of the exponential $N\psi(\sqrt{2V}a_N)$ in (46) to be $O(1)$, where $\sqrt{2V}$ is a trivial scaling due to the form of $\psi(w|V)$ in (32). From (32), this means $a_N \sim \sqrt{\ln N}$. Therefore, for large N , the maximum value scales as $M_1 = \sqrt{2V}(a_N + b_N z)$, where $\sqrt{2V}b_N$ denotes the strength of the fluctuations and z is a random variable describing the PDF of the fluctuations around $\sqrt{2V}a_N$. Using $\psi(w)$ from (32) and taking the limit $N \rightarrow \infty$ we arrive at the Gumbel distribution [30–33]

$$\lim_{N \rightarrow \infty} \text{Prob.}(M_1 < w = \sqrt{2V}(a_N + b_N z)|V) \rightarrow e^{-e^{-z}}. \quad (47)$$

In order for the right hand side of (47) to be independent of N , the parameters a_N and b_N , must satisfy the following relations

$$a_N = \text{erfc}^{-1}(2/N) \sim \sqrt{\ln N} \quad \text{and} \quad b_N = \frac{\sqrt{\pi}}{N} e^{a_N^2} \sim \frac{1}{2\sqrt{\ln N}}. \quad (48)$$

The strength of the fluctuation $b_N \rightarrow 0$ as $N \rightarrow \infty$, and therefore, to the leading order, one can neglect the fluctuations and get

$$\text{Prob.}(M_1 = w|V) = \delta(w - \sqrt{2V}a_N). \quad (49)$$

The unconditional distribution for the extreme value M_1 is given by

$$\text{Prob.}(M_1 = w) = \int_0^\infty dV h(V, t) \text{Prob.}(M_1 = w|V). \quad (50)$$

Therefore, using (11) and (49) in (50), we get

$$\text{Prob.}(M_1 = w) = \int_0^\infty \frac{dV}{[\xi(t)]^2} Q\left(\frac{V}{\xi(t)}\right) \delta(w - \sqrt{2V}a_N) = \frac{w}{[a_N \xi(t)]^2} Q\left(\frac{w^2}{2[a_N \xi(t)]^2}\right). \quad (51)$$

Therefore, the PDF of the maximum M_1 in (51) is a special case of the order statistics in (39) with $\alpha = 1/N$, as a_N defined in (48) is the same as $\theta_{1/N}$ defined in (39).

6. Gap statistics

While the order statistics describes the position fluctuations of individual ordered particles, the gap statistics describes the statistics of separations between successive ordered particles. Let $d_k(V) = M_k(V) - M_{k+1}(V)$ denotes the gap between the k -th and $(k+1)$ -th ordered particles, for a given realization of V . Then the unconditional gap statistics is given by

$$\text{Prob.}(d_k = g) = \int_0^\infty dV h(V, t) \text{Prob.}(M_k(V) - M_{k+1}(V) = g). \quad (52)$$

The conditional PDF $\text{Prob.}(M_k(V) - M_{k+1}(V) = g)$ can be obtained from the joint distribution of M_k and M_{k+1} for a given V [1],

$$\begin{aligned} \text{Prob.}[M_k(V) = x, M_{k+1}(V) = y] &= \frac{N!}{(k-1)!(N-k-1)!} p(x|V)p(y|V) \\ &\times [\psi(x|V)]^{k-1} [1 - \psi(y|V)]^{N-k-1} \theta(x - y). \end{aligned} \quad (53)$$

The distribution of the gap $d_k(V) = M_k(V) - M_{k+1}(V)$ for a given V is then is given by

$$\text{Prob.}(M_k(V) - M_{k+1}(V) = g) = \int_{-\infty}^\infty \text{Prob.}[M_k(V) = y + g, M_{k+1}(V) = y] dy. \quad (54)$$

Starting with the joint distribution in (53) and going via (54), in the large N limit, one finds that [1, 2]

$$\text{Prob.}(M_k(V) - M_{k+1}(V) = g|V) \approx N p(q|V) e^{-N p(q|V) g}, \quad (55)$$

where $q \equiv q(\alpha, V) = \sqrt{2V} \text{erfc}^{-1}(2\alpha)$ defined in equation (35). Finally, averaging equation (55) over $h(V, t)$, as in (52), and using the scaling form in (11) and $p(x|V)$ in (31), we get

$$\text{Prob.}(d_k = g) = \frac{1}{\lambda_N(t)} F\left(\frac{g}{\lambda_N(t)}\right), \quad (56)$$

where $\lambda_N(t) = \sqrt{2\pi} \xi(t) e^{\theta_\alpha^2}/N$ with $\theta_\alpha = \operatorname{erfc}^{-1}(2\alpha)$ and the scaling function $F(z)$ is given by

$$F(z) = \int_0^\infty du Q(u) \frac{e^{-z/\sqrt{u}}}{\sqrt{u}}. \quad (57)$$

Using the expression (14) for $Q(z)$, the integral in (57) can be performed explicitly, which gives,

$$F(z) = \frac{2\sqrt{2}}{\sqrt{\pi}} \sum_{n=0}^{\infty} \binom{-\frac{1}{2}}{n} \frac{1}{c_n} \left[1 - \frac{\sqrt{\pi} z e^{z^2/c_n^2}}{c_n} \operatorname{erfc}\left(\frac{z}{c_n}\right) \right] \quad \text{with } c_n = 4n + 1. \quad (58)$$

The two infinite sums are individually convergent, and the first can be explicitly evaluated,

$$F(z) = \frac{[\Gamma(1/4)]^2}{2\sqrt{2}\pi} - 2\sqrt{2} \sum_{n=0}^{\infty} \binom{-\frac{1}{2}}{n} \frac{z e^{z^2/c_n^2}}{c_n^2} \operatorname{erfc}\left(\frac{z}{c_n}\right). \quad (59)$$

The scaling function $F(z)$ has support over the positive real line. It describes the gap statistics in the bulk as well as the edge. We compare this analytical result with numerical simulations in figure 5 and find excellent agreement. The function $F(z)$ approaches a constant as $z \rightarrow 0$,

$$F(0) = \frac{[\Gamma(1/4)]^2}{2\sqrt{2}\pi} = 1.47933\dots \quad (60)$$

and has a linear decay for small z ,

$$F(z) = F(0) - F_1 z + O(z^2) \quad \text{with } F_1 = 2.78143\dots \quad (61)$$

This behavior indicates that there is no effective repulsion between the particles.

Let us now find the tail behavior of $F(z)$. Because of the presence of the essential singularity $e^{-z/\sqrt{u}}$ in the integral in (57), the integrand contributes substantially only for $u \gtrsim z^2$. Therefore, for large z , the dominant contribution to the integral in (57) comes from the tail behavior of $Q(u)$. Using the large u asymptotic form (15) for $Q(u)$ in (57), we get

$$F(z) = \frac{1}{2} \int_0^\infty dz \frac{1}{u} e^{-u\pi^2/16} e^{-z/\sqrt{u}} \sim \frac{2\pi^{1/6}}{\sqrt{3} z^{1/3}} e^{-\frac{3}{4}(\pi z)^{2/3}}. \quad (62)$$

This stretched exponential tail behavior $F(z)$ in (62) for large z is similar to that observed for the resetting Brownian motion [1], originating from the exponential tail of $Q(u)$ in both cases.

7. Full Counting Statistics

Finally, we consider the full counting statistics (FCS), which describes the probability distribution of the number of particles in a given region in space. For simplicity, here, we consider the region $[-L, L]$. For a given V , since the conditional JPDF of the positions

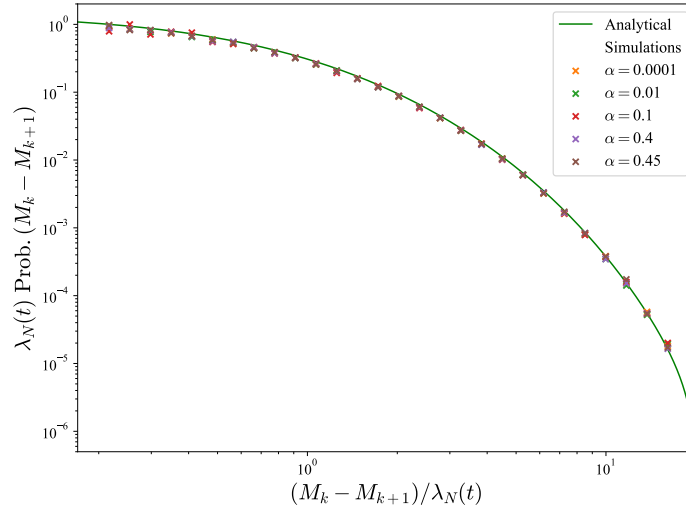


Figure 5. Plot of the distribution of the scaled spacing variable $(M_k - M_{k+1})/\lambda_N(t)$. The points are from numerical simulations while the solid line plots (59). The parameters used in the simulation are $\Lambda = 1$, $t = 4$, $N = 10^6$, and averaged over 10^6 realizations.

in (4) have the product form, the probability of finding N_L particles in between $[-L, L]$, for a given V , is simply the binomial distribution,

$$\text{Prob.}(N_L, N|V) = \binom{N}{N_L} \left[\int_{-L}^L dx p(x|V) \right]^{N_L} \left[1 - \int_{-L}^L dx p(x|V) \right]^{N-N_L} \quad (63)$$

In the asymptotic limit, we expect N_L to be large for any non-zero L . Therefore, setting $N_L = \kappa N$ with $\kappa \in [0, 1]$, we note that for large N , the binomial distribution converges to the Gaussian distribution with mean $\langle N_L \rangle$ and variance $\langle N_L^2 \rangle_c$ given by,

$$\langle N_L \rangle = N \int_{-L}^L dx p(x|V), \quad (64)$$

$$\langle N_L^2 \rangle_c = N \left[\int_{-L}^L dx p(x|V) \right] \left[1 - \int_{-L}^L dx p(x|V) \right]. \quad (65)$$

Consequently, the relative fluctuations scale as $\sqrt{\langle N_L^2 \rangle_c} / \langle N_L \rangle \sim N^{-1/2}$ and in the limit $N \rightarrow \infty$, the distribution for the fraction of particles κ in $[-L, L]$ converges to a Dirac delta function about

$$\int_{-L}^L dx p(x|V) = \text{erf} \left(\frac{L}{\sqrt{2V}} \right).$$

Hence, the the probability distribution of N_L , which can be found by averaging $\text{Prob.}(N_L, N|V)$ with respect to V using (11), has the scaling form

$$\text{Prob.}(N_L, N, t) = \frac{1}{N} H \left(\frac{N_L}{N}, t \right), \quad (66)$$

where the scaling function $H(\kappa, t)$ describing the PDF the fraction of particles κ in $[-L, L]$ at time t is given by

$$H(\kappa, t) = [\xi(t)]^{-2} \int_0^\infty dV Q(V/[\xi(t)]^2) \delta \left[\kappa - \operatorname{erf} \left(\frac{L}{\sqrt{2V}} \right) \right]. \quad (67)$$

Performing the above integral leads to,

$$H(\kappa, t) = \frac{\sqrt{\pi}}{2[\ell(t)]^2} \frac{\exp[\operatorname{erf}^{-1}(\kappa)^2]}{[\operatorname{erf}^{-1}(\kappa)]^3} Q \left(\frac{1}{[\sqrt{2}\ell(t)\operatorname{erf}^{-1}(\kappa)]^2} \right), \text{ with } \ell(t) = \frac{\xi(t)}{L} \propto t, \quad (68)$$

where $\xi(t) = \sqrt{2}\Lambda t$, is defined in (11). The distribution in (68) is supported over the entire range $[0, 1]$. Using $\operatorname{erf}^{-1}(\kappa) = \sqrt{\pi}\kappa/2 + O(\kappa^2)$ as $\kappa \rightarrow 0$ and the asymptotic form of $Q(z)$ from (15) in (68) one finds,

$$H(\kappa, t) = \sqrt{\frac{2}{\pi}} \frac{1}{\ell(t)\kappa^2} \exp \left[-\frac{\pi}{8[\ell(t)]^2\kappa^2} \right] \text{ as } \kappa \rightarrow 0. \quad (69)$$

Thus, the distribution has an essential singularity at the lower support $\kappa = 0$. Since all the particles start from the origin, the probability of finding no particles inside the domain $[-L, L]$ is evidently zero at $t = 0$. As time progresses, since the gas expands ballistically, more and more particles leave the finite domain $[-L, L]$. This is reflected in the scale at which the essential singularity manifests in (69), which decreases with time as $1/\ell(t) \sim 1/t$.

On the other hand, for $\kappa \rightarrow 1$ from below, using $\operatorname{erf}^{-1}(\kappa) \sim \sqrt{-\ln[1-\kappa]}$ and the small z behavior of $Q(z)$ from (16), we get

$$H(\kappa, t) = \ell(t)(1-\kappa)^{\beta(t)} \text{ with } \beta(t) = \frac{[\ell(t)]^2}{2} - 1 = \left(\frac{\Lambda}{L} \right)^2 t^2 - 1. \quad (70)$$

Thus near the upper support $\kappa = 1$, the scaling function $H(\kappa, t)$ has a rather unusual behavior: $H(\kappa, t) \sim (1-\kappa)^{\beta(t)}$ where the exponent $\beta(t)$ changes continuously with time. The scaling function $H(\kappa, t)$ undergoes an interesting dynamic shape transition near the upper support $\kappa = 1$ with time. At early times $t < t_c = L/\Lambda$, the exponent $\beta(t) < 0$ and consequently, there is a power law divergence of $H(\kappa, t)$ near $\kappa = 1$, while for $t > t_c$, $H(\kappa, t) \rightarrow 0$ as $\kappa \rightarrow 1$. At the transition time $t = t_c$, the function $H(\kappa, t_c)$ becomes flat and converges to a non-zero value as $\kappa \rightarrow 1$. This is because, since the gas is initially localized at the origin, all the particles are within $[-L, L]$ at $t = 0$. As time progresses, particles leave the region. The time $t_c = L/\Lambda$ is indeed the typical time needed for a particle to hit the boundary L starting at the origin. The above results are verified by the simulations presented in figure 6.

8. Conclusion

In this paper, we have studied a gas of N Brownian particles subjected to a common stochastic diffusivity $D(t) = B^2(t)$, where $B(t)$ is another independent Brownian motion

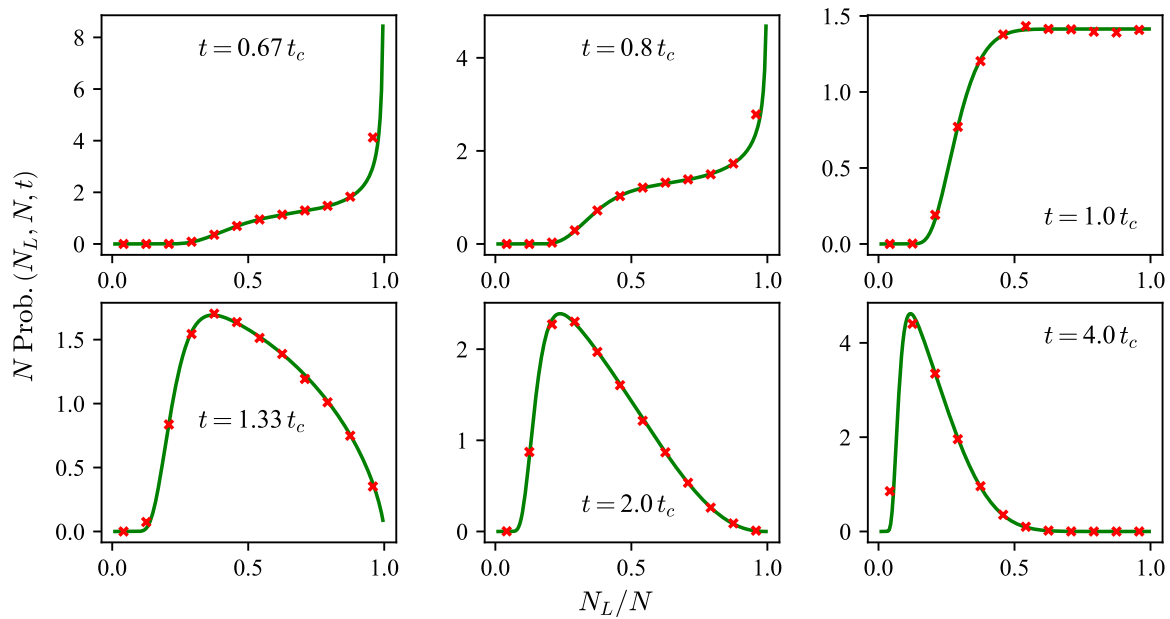


Figure 6. The PDF of the fraction of particles $H(N_L/N, t) = N \text{Prob.}(N_L/N, t)$. The markers are of numerical simulations with parameters $\Lambda = 1$, $N = 3 \times 10^5$, averaged over 2×10^5 realizations. The solid lines plots the function $H(N_L/N, t)$ given in (68). We see that the curve flattens near $N_L/N = 1$ for $t = t_c = L/\Lambda$. For times less than t_c , the probability density approaches zero, while for times greater than t_c , there is a power-law divergence at the upper support.

with a constant diffusion coefficient. We start with the initial condition where the gas is localized at the origin. The gas expands ballistically over time with a length scale $\xi(t) \propto t$, and we obtained the exact joint probability density function (JPDF) of the position of all the particles at all times t . We have shown that there is a dynamically generated all-to-all attraction between particles at any finite $t > 0$, even though there is no direct interaction between the particles. Moreover, we have shown that the JPDF at any finite time t , though not factorizable into individual marginal distributions, indicating strong non-zero correlations, has a special conditionally independent and identically distributed (CIID) structure. This CIID structure allows us to compute several macroscopic and microscopic observables exactly at all times t , despite the presence of strong correlations at finite time $t > 0$. These observables include the average density profile of the gas, the extreme and the order statistics of the positions of the particles, the distribution of the spacing between two consecutive particles, and also the full counting statistics, i.e., the distribution of the number of particles in an interval $[-L, L]$. They exhibit a rich variety of interesting behaviors.

In this paper, we have used the choice of the fluctuating diffusivity $D(t) = B^2(t)$. It would be interesting to study other choices of stochastic diffusivity, such as the square of an Ornstein-Uhlenbeck process. It would also be interesting to study such dynamically correlated gas in a confining potential. Finally, here we have considered a gas where

there are no direct interactions between the particles. It would be interesting to extend this study, where there is already a direct interaction between the particles, and then subject the system to a common fluctuating environment, as in some of the recent studies [23, 24].

9. Acknowledgements

SNM and SS acknowledge the support from the Science and Engineering Research Board (SERB, Government of India), under the VAJRA faculty scheme No. VJR/2017/000110. SNM acknowledge the ANR Grant No. ANR- 23- CE30-0020-01 EDIPS. SNM and SS thank the support from the International Research Project (IRP) titled ‘Classical and quantum dynamics in out of equilibrium systems’ by CNRS, France. SS thanks the hospitality of Laboratoire de Physique Théorique et Modèles Statistiques (LPTMS) and Laboratoire de Physique Théorique et Hautes Energies (LPTHE), Sorbonne Université, Paris, France.

References

- [1] Biroli M, Larralde H, Majumdar S N and Schehr G 2023 Extreme statistics and spacing distribution in a Brownian gas correlated by resetting *Phys. Rev. Lett.* **130** 207101 URL <https://link.aps.org/doi/10.1103/PhysRevLett.130.207101>
- [2] Biroli M, Larralde H, Majumdar S N and Schehr G 2024 Exact extreme, order, and sum statistics in a class of strongly correlated systems *Phys. Rev. E* **109** 014101 URL <https://link.aps.org/doi/10.1103/PhysRevE.109.014101>
- [3] Biroli M, Kulkarni M, Majumdar S N and Schehr G 2024 Dynamically emergent correlations between particles in a switching harmonic trap *Phys. Rev. E* **109** L032106 URL <https://link.aps.org/doi/10.1103/PhysRevE.109.L032106>
- [4] Sabhapandit S and Majumdar S N 2024 Noninteracting particles in a harmonic trap with a stochastically driven center *J. Phys. A: Math. Theor.* **57** 335003 URL <https://dx.doi.org/10.1088/1751-8121/ad6651>
- [5] Biroli M, Ciliberto S, Kulkarni M, Majumdar S N and Schehr G (unpublished)
- [6] Kulkarni M, Majumdar S N and Sabhapandit S 2025 Dynamically emergent correlations in bosons via quantum resetting *J. Phys. A: Math. Theor.* **58** 105003 URL <https://dx.doi.org/10.1088/1751-8121/adb6db>
- [7] Chubynsky M V and Slater G W 2014 Diffusing diffusivity: A model for anomalous, yet Brownian, diffusion *Phys. Rev. Lett.* **113** 098302 URL <https://link.aps.org/doi/10.1103/PhysRevLett.113.098302>
- [8] Chechkin A V, Seno F, Metzler R and Sokolov I M 2017 Brownian yet non-gaussian diffusion: from superstatistics to subordination of diffusing diffusivities *Phys. Rev. X* **7** 021002
- [9] Tyagi N and Cherayil B J 2017 Non-gaussian Brownian diffusion in dynamically disordered thermal environments *J. Phys. Chem. B* **121** 7204
- [10] Lanoiselée Y and Grebenkov D S 2018 A model of non-gaussian diffusion in heterogeneous media *J. Phys. A: Math. Theor.* **51** 145602
- [11] Sposini V, Grebenkov D S, Metzler R, Oshanin G and Seno F 2020 Universal spectral features of different classes of random-diffusivity processes *New J. Phys.* **22** 063056
- [12] Barkai E and Burov S 2020 Packets of diffusing particles exhibit universal exponential tails *Phys. Rev. Lett.* **124** 060603

- [13] Pacheco-Pozo A and Sokolov I M 2021 Large deviations in continuous-time random walks *Phys. Rev. E* **103** 042116
- [14] Hamdi O, Burov S and Barkai E 2024 Laplace’s first law of errors applied to diffusive motion *Eur. Phys. J. B* **97** 1
- [15] Singh R and Burov S 2024 The emergence of laplace universality in correlated processes *arXiv preprint arXiv:2410.23112*
- [16] Guéneau M, Majumdar S N and Schehr G 2025 Large deviations in switching diffusion: from free cumulants to dynamical transitions *arXiv preprint arXiv:2501.13754*
- [17] Hidalgo-Soria M, Barkai E and Burov S 2021 Cusp of non-gaussian density of particles for a diffusing diffusivity model *Entropy* **23** 231
- [18] Sposini V, Chechkin A and Metzler R 2018 First passage statistics for diffusing diffusivity *J. Phys. A: Math Theor* **52** 04LT01
- [19] Jain R and Sebastian K 2017 Diffusion in a crowded, rearranging environment *J. Chem. Phys.* **146** 214102
- [20] Jain R and Sebastian K L 2016 Diffusing diffusivity: survival in a crowded rearranging and bounded domain *J. Phys. Chem. B* **120** 9215
- [21] Yin Q, Li Y, Marchesoni F, Nayak S and Ghosh P K 2021 Non-gaussian normal diffusion in low dimensional systems *Front. Phys.* **16** 1
- [22] Santra I, Basu U and Sabhapandit S 2022 Effect of stochastic resetting on brownian motion with stochastic diffusion coefficient *J. Phys. A: Math. Theor.* **55** 414002 URL <https://dx.doi.org/10.1088/1751-8121/ac8dcc>
- [23] Dean D S, Majumdar S N and Sabhapandit S 2025 Exact height distribution in one-dimensional edwards–wilkinson interface with diffusing diffusivity *J. Phys. A: Math. Theor.* **58** 235002 URL <https://dx.doi.org/10.1088/1751-8121/add8cd>
- [24] Biroli M, Majumdar S N and Schehr G 2025 Resetting dyson brownian motion *arXiv preprint arXiv:2503.14733*
- [25] Cameron R H and Martin W T 1944 The wiener measure of hilbert neighborhoods in the space of real continuous functions *Journal of Mathematics and Physics* **23** 195
- [26] Cameron R and Martin W 1945 Transformations of wiener integrals under a general class of linear transformations *Transactions of the American Mathematical Society* **58** 184–219
- [27] Erdős P and Kac M 1946 On certain limit theorems of the theory of probability *Bull. Amer. Math. Soc.* **52** 292 URL <http://dml.mathdoc.fr/item/1183507847>
- [28] Kac M 1949 On distributions of certain wiener functionals *Transactions of the American Mathematical Society* **65** 1
- [29] Santra I, Basu U and Sabhapandit S 2021 Active Brownian motion with directional reversals *Phys. Rev. E* **104** L012601 URL <https://link.aps.org/doi/10.1103/PhysRevE.104.L012601>
- [30] Sabhapandit S, Majumdar S N and Redner S 2008 Crowding at the front of marathon packs *J. Stat. Mech.* **2008** L03001 URL <https://dx.doi.org/10.1088/1742-5468/2008/03/L03001>
- [31] Majumdar S N, Pal A and Schehr G 2020 Extreme value statistics of correlated random variables: a pedagogical review *Phys. Rep.* **840** 1
- [32] Majumdar S N and Schehr G 2024 *Statistics of Extremes and Records in Random Sequences* (Oxford University Press)
- [33] Sabhapandit S 2019 Extremes and records *arXiv preprint arXiv:1907.00944*